Journal of Applied Polymer Science

Synergistic Effects of β-Modification and Impact Polypropylene Copolymer on Brittle-Ductile Transition of Polypropylene Random Copolymer

Yanling Zhu, Feng Luo, Hongwei Bai, Ke Wang, Hua Deng, Feng Chen, Qin Zhang, Qiang Fu
Department of Polymer Science and Engineering, College of Polymer Science and Engineering,
State Key Laboratory of Polymer Materials Engineering, Sichuan University, Chengdu 610065, People's Republic of China
Correspondence to: Q. Fu (E-mail: qiangfu@scu.edu.cn)

ABSTRACT: In this work, the synergistic effects of β-modification and impact polypropylene copolymer (IPC) on brittle–ductile (B–D) transition behavior of polypropylene random copolymer (PPR) have been investigated. It is interesting to find that adding both IPC and β-nucleating agent into PPR has three effects: (i) leading to a significant enhancement in β-crystallization capability of PPR, (ii) contributing to the shift of B–D transition to lower temperatures, (iii) increasing the B–D transition rate. The reason for these changes can be interpreted from the following two aspects. On one hand, the transition of crystalline structure from α-form to β-form reduces the plastic resistance of PPR matrix, thus causing the initiation of matrix shear yielding much easier during the impact process. On the other hand, the well dispersed rubbery phase in IPC with high molecular mobility at relatively low temperatures is beneficial to the shear yielding of PPR matrix and, subsequently, the great improvement in impact toughness of the ternary blends. © 2013 Wiley Periodicals, Inc. J. Appl. Polym. Sci. 129: 3613–3622, 2013

KEYWORDS: blends; crystallization; morphology; structure–property relations

Received 5 December 2012; accepted 30 January 2013; published online 1 March 2013
DOI: 10.1002/app.39107

INTRODUCTION

Nowadays, polypropylene random copolymer (PPR) has been widely used as matrix component in pipe, automobile parts, furniture, and other industrial uses owing to its outstanding comprehensive properties and relative low cost.[1–4] However, in many special occasions, its application has been greatly hindered by its insufficient low-temperature toughness.[5] Thus, great research efforts has been made in recent years to toughen PPR, such as adding inorganic fillers (cenosphere,[6] wollastonite,[7] ceramic particles[8]), fibers,[9,10] and elastomers[11,12] or rubbers.[13] Of these methods blending PPR with thermoplastic elastomers is most effective to obtain a high level of low-temperature toughness. Nevertheless, such improvement of toughness is at the cost of sacrificing strength and modulus.[14,15] Very interestingly, it has been widely demonstrated that β-form PP exhibits a much higher toughness and a similar strength and stiffness as compared with the common α-form PP.[16–21] Unfortunately, the polymorphic behavior of PPR is very difficult to be tailored even in the presence of highly active nucleating agents because of its random copolymer chain configuration, so it is impractical to toughen PPR only by adding β-nucleating agent (β-NA).[22–26]

In polymer materials, normally there is a typical brittle–ductile (B–D) transition, which is the sharp shift in the failure mode from brittle fracture with poor impact toughness to ductile fracture with good impact toughness with increasing testing temperature.[27] The B–D transition curve provides a very important information for evaluating the toughness of the polymers from industrial points of view. Many previous investigations have identified that B–D transition behaviors of polypropylene (PP)/elastomer blends not only depend on the dispersed elastomer phase, but also depend on the matrix properties such as crystalline structure and morphology.[28–32] The presence of large amounts of β-form crystals in the PP matrix is favorable to the shift of B–D transition towards lower temperatures.[33] Therefore, a notable decrease in B–D transition temperature of PPR matrix with soft rubber phase will be expected if extensive β-form crystals could be formed in the matrix.

In our previous work, it is very interesting to find that isotactic polypropylene (iPP) plays an important role in improving the β-crystallization capability of β-nucleated PPR.[34] Inspired by this idea, we further selected IPC to substitute iPP for the toughening of PPR. It is expected that an excellent low-temperature toughness of PPR could be obtained by adding IPC and

β-NA simultaneously, while almost maintain constant stiffness and strength. The reason for choosing IPC rather than iPP is that, IPC not only exhibits a great potential to significantly enhance the content of β-form crystals in PPR matrix due to its high chain stereoregularity like iPP, but also shows a much better toughness at low temperature in comparison with iPP.[17]

This work mainly focus on the synergistic toughening effects of IPC and β-nucleating agent on PPR, with a special attention on the effects of IPC content and β-nucleating agent content on the B–D transition behavior. Many measurements including wide angle X-ray diffraction (WAXD), dynamic mechanical analysis (DMA), and scanning electron microscopy (SEM) are employed to uncover the toughening mechanism.

EXPERIMENTAL

Materials and Sample Preparation

The polypropylene random copolymer (PPR) (trade name R200P, $M_w = 72.2\times10^4$ g mol^{-1}, density = 0.91 g cm^{-3}) used as the matrix was supplied by Hyosung (Korea). The weight percentage of ethylene component is about 3.8 wt%. The commercial grade Impact polypropylene copolymer (IPC) (trade name SP179, $M_w = 1.74\times10^5$ g.mol^{-1}, $M_w/M_n = 3.96$, density = 0.91 g.cm^{-3}) was produced by Qilu petrochemical Co. (China). The weight percentage of ethylene component is about 13.5 wt%. The β-nucleating agent (trade name WBG) is a rare earth agent composed of hetero-nuclear dimetal complexes of lanthanum and calcium containing some specific ligands. It was kindly provided by Guangdong Winner Functional Materials Co. (Foshan, China).

The PPR/IPC/WBG blends used in this work were prepared as follows. First, the pure PPR and WBG powders were melt-mixed by a TSSJ-25 corotating twin screw extruder (china) to obtain the master-batch of 5 wt % WBG in PPR. Then, the master-batch was melt blended with different contents of PPR and IPC by using the extruder. After making pellets and drying at 80°C, the standard specimens were molded on an injection machine (PS40E5ASE, Japan). The barrel temperature and mould temperature were set as 210 and 30°C, respectively. For convenience, the samples were designated as R/xC/yG, where R, C, and G represent PPR, IPC, and WBG, respectively; the x and y indicate the weight percentage of IPC and WBG, respectively. For example, R/10C/0.05G means the PPR/IPC/WBG blend with 10 wt % IPC and 0.05 wt % WBG.

Characterization and Measurements

Mechanical Properties. The notched Izod impact strength was measured at −20∼ 50°C with a VJ-40 Izod machine according to ASTM D256-04 standard. For each sample, the average value was based on at least six specimens. The tensile testing was carried out at room temperature (23°C) with an SANS Universal tensile testing machine in accordance with ASTM D638-03 standard.

Wide Angle X-ray Diffraction. The WAXD spectra were recorded with a Philips X'Pert pro MPD apparatus in the 2θ range of 5–40° (5°/min). The measurement was performed using a conventional Cu Kα X-ray ($\lambda = 0.154$ nm, reflection mode) tube at a voltage of 40 kv and a filament current of 40 mA. The crystallinity (X_c) of the samples was calculated according to the following equation:

$$X_c = \frac{\sum A_{\text{cryst}}}{\sum A_{\text{cryst}} + \sum A_{\text{amorp}}} \times 100\% \quad (1)$$

where A_{cryst} and A_{amorp} represent for the integral intensities of crystalline and amorphous regions, respectively.

The relative amount of β-form crystals (K_β) was evaluated according to the method proposed by Turner-Jones et al.[35]

$$K_\beta = \frac{A_\beta(300)}{A_\alpha(110) + A_\alpha(040) + A_\alpha(130) + A_\beta(300)} \times 100\% \quad (2)$$

where $A_\beta(300)$ are the intensity of the (300) reflection peak of β-form crystal at 2θ=16.1°, and $A_\alpha(110)$, $A_\alpha(040)$, $A_\alpha(130)$ are the intensities of the (110), (040), and (130) reflection peaks of α-form crystal at 14.1°, 16.9°, and 18.6°, respectively.

Scanning Electron Microscopy. The microscopic phase morphologies and the impact-fractured surfaces of the samples were observed with an FEI Inspect F SEM instrument at an acceleration voltage of 20 kv. Specimens for the SEM observation of the phase morphology were prepared by the cryogenic fracture of the injection molded bars under liquid nitrogen and the subsequent chemical etch of the amorphous EPR phase by xylene. In order to observe that crystalline structure, the cryo-fractured surface was etched in the mixed liquid of sulfuric acid, phosphoric acid, and potassium permanganate. All the samples were sputter-coated with a thin layer of gold before the observations.

Dynamic Mechanical Analysis. The dynamic mechanical analysis was performed using a DMA Q800 analyzer (TA instruments, USA). The single cantilever mode was applied and the measurement was carried out on a rectangular molded bar with dimensions of 30 mm × 10.2 mm × 4.2 mm (length × wide × thickness) from −100°C to 120°C at a heating rate of 3°C/min and an oscillatory frequency of 1 Hz.

RESULTS AND DISCUSSION

Synergistic Toughening Effect of β-NA and IPC on PPR

Figure 1(a) shows the variation of notched Izod impact strength of PPR and R/10C blends with and without 0.05 wt % WBG as a function of testing temperature (−20∼50°C). As expected, a typical B–D transition in impact strength can be clearly observed in all of the samples. Compared with pure PPR, R/10C blend exhibits not only a slight shift of B–D transition towards lower temperature but also a much more evident B–D transition. As the testing temperature exceeds a certain value (around 3°C), the impact strength increases rapidly. For the sample of R/0.05G, the B–D transition curve is found to be similar to that of R/10C blend. In the investigated temperature range, there is only a small difference in the impact toughness between them. More interestingly, it is evident that IPC and β-NA have a synergistic toughening effect on PPR, even in the low temperature range. As shown in Figure 1(b), at the testing temperature of 0°C, the impact strength of R/10C and R/0.05G blends is 7.8 kJ/m^2 and 8.8 kJ/m^2, respectively. However, once

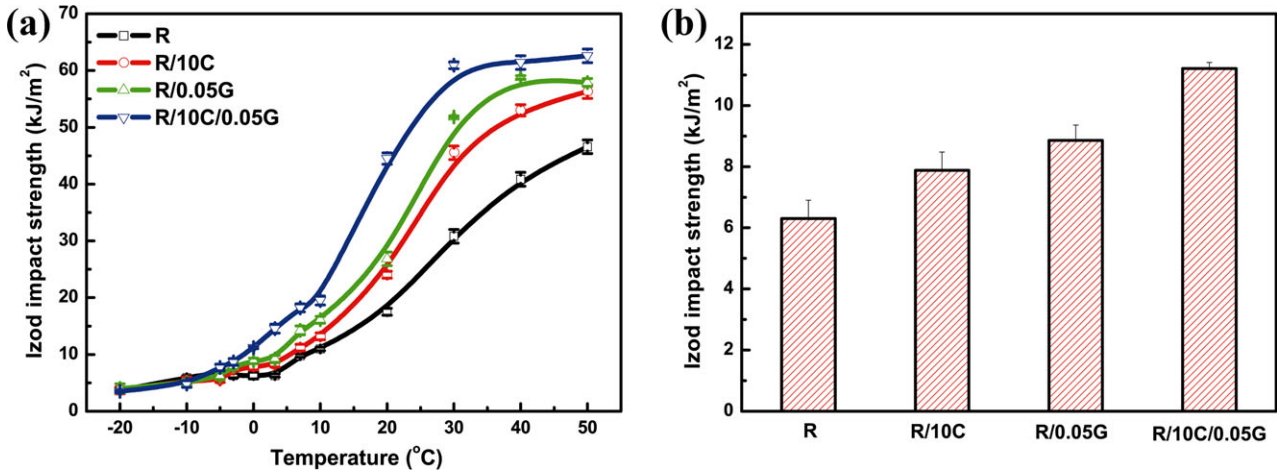

Figure 1. (a) Brittle–ductile transition curves and (b) notched Izod impact strength measured at 0°C for PPR, PPR/10IPC, PPR/0.05WBG, and PPR/10IPC/0.05WBG. [Color figure can be viewed in the online issue, which is available at wileyonlinelibrary.com.]

0.05 wt % WBG and 10 wt % IPC are simultaneously introduced into PPR, the R/10C/0.05G blend displays a great improvement in impact toughness. The impact strength increases from 6.3 kJ/m^2 of pure PPR to 11.2 kJ/m^2, about two times in improvement. Furthermore, the B–D transition temperature of R/10C/0.05G blend depresses about 8°C in comparison with that of pure PPR.

To explore the fracture mechanism of R/10C/0.05G blend during the impact process at different testing temperatures, some typical impact fracture surfaces were characterized via SEM and the results are presented in Figure 2. For the sample tested at −20°C, the impact fracture surface is quite smooth and the weak plastic deformation can only be observed in the region of crack initiation, indicating a typical brittle fracture mode. With the increase of testing temperature, the area of the plastic deformation zone enlarges significantly [Figure 2(a,b)]. For the sample tested at 20°C, the shear yielding or plastic deformation prevails throughout the whole impact fracture surface [Figure 2(c)]. More interestingly, besides the shear yielding of PPR matrix, both the striations and fibrils are clearly observed in the sample tested at 40°C [Figure 2(d)], implying that the fracture process involves a severe plastic deformation. Based on the above observations, it is very clear that the fracture mode of PPR matrix changes from brittle multiple crazing into extensive shear yielding with increasing test temperature, which causes the B–D transition.

Polycrystalline Composition and Phase Morphology

Above results demonstrate the synergistic toughening effect of β-NA and IPC on PPR. Since PP is a polymorphic material and the crystalline structure plays an important role in the

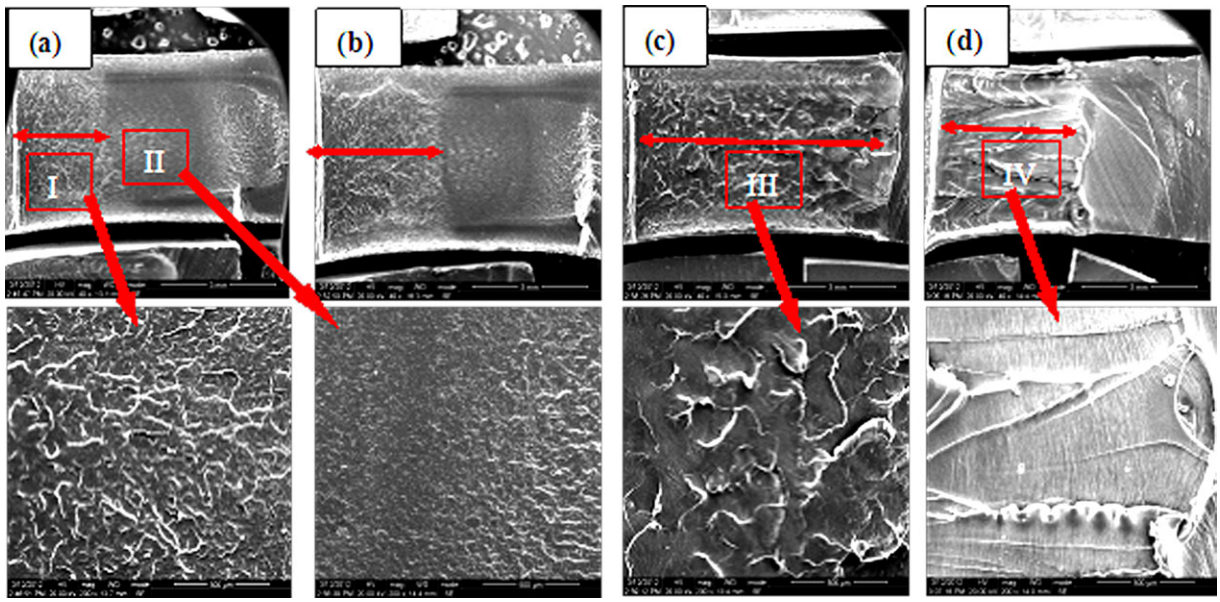

Figure 2. Impact fracture surface of PPR/10IPC/0.05WBG measured at different temperatures: (a) −20°C, (b) 0°C, (c) 20°C, and (d) 40°C. [Color figure can be viewed in the online issue, which is available at wileyonlinelibrary.com.]

Applied Polymer SCIENCE

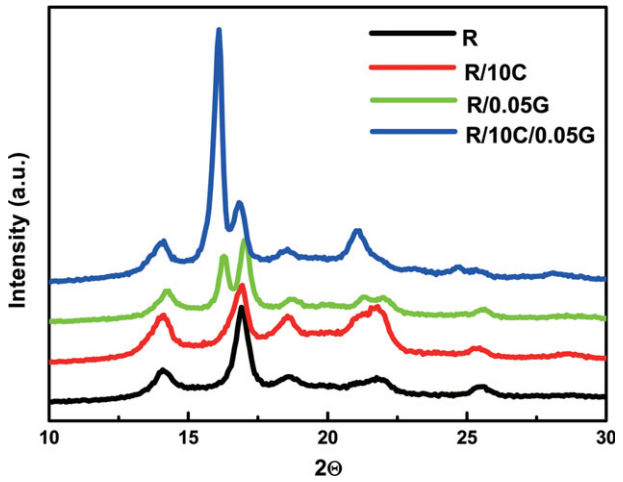

Figure 3. WAXD spectra of PPR, PPR/10IPC, PPR/0.05WBG, and PPR/10IPC/0.05WBG. [Color figure can be viewed in the online issue, which is available at wileyonlinelibrary.com.]

toughening, the polycrystalline composition of PPR matrix in the R/10C blend with and without WBG was characterized by WAXD and the results are shown in Figure 3 and Table I. Clearly, no any β-form crystals can be detected in pure PPR and R/10C blend. With regard to the blend of R/0.05G, some β-form crystals are induced by 0.05 wt % WBG as expected. However, in this case, the relative amount of β-form crystals is just 34%, which is much lower than that in iPP with 0.05 wt % WBG (as reported in our previous work).[36] Importantly, it is very interesting to find that, with the introduction of 10 wt % IPC into the R/0.05G blend, the relative amount of β-form crystals significantly increases up to 72%, indicating that IPC can effectively enhancing the nucleating effect of β-NA in PPR matrix crystallization. Additionally, the crystallinity of R/10C/0.05G blend is found to be comparable to that of R/10C and R/0.05G blends.

The microstructures of the blends were investigated by SEM. In the SEM micrographs, the dark holes represent the dispersed EPR phase, which was etched out from the samples by xylene. As shown in Figure 4(a), pure PPR exhibits a sea-island phase morphology with dispersed EPR phase. Because of the multiphase nature of IPC, the addition of IPC into PPR not only introduces some relatively big rubbery particles but also increase the number of the relatively small rubbery particles [Figure 4(b)]. The phase morphology and crystalline structure of R/0.05G blend are significantly different from that of pure PPR. First, the EPR domains are much smaller and more uniform probably because of the strong suppressing effect of β-NA induced accelerated crystallization of PPR matrix on the phase separation [Figure 4(c)]. Second, it can be clearly observed that some β-form crystals are formed in the PPR matrix after adding β-NA WBG. For the ternary blend of R/10C/0.05G, the dispersed rubbery phase is well-distributed and the PPR matrix is almost completely occupied by the nucleated β-form crystals [Figure 4(d)]. Considering the variations of impact toughness, polycrystalline composition and phase morphology of R/10C blend when β-NA is added into the blend, it is believed that the exclusive formation of β-form crystals and the increase of rubbery phase concentration are the main reason for the synergetic toughening effects of WBG and IPC on PPR.

Mechanical Properties of PPR/IPC/WBG Blends as a Function of IPC Content and WBG Content

In order to further study the effects of IPC content and β-NA content on the impact toughness of PPR/IPC/WBG blends, the B–D transition curves of the samples have been investigated. As shown in Figure 5(a), the B–D transition curves of PPR/IPC blends gradually shift to lower temperatures with increasing IPC content. For example, the B–D transition temperature decreases from 3°C of pure PPR to −10°C of R/30C blend. On the other hand, at a given testing temperature, the Izod impact strength improves significantly with the increase of IPC content from 10 to 40 wt %. However, it should be noted that no effective toughening can be observed when the testing temperature is below than −10°C. Similarly, although addition of small amounts (0.1∼ 0.2 wt %) of β-NA into R/10C blends can induce an obvious shift of the B–D transition temperature towards lower temperature and an dramatic enhancement in the impact toughness at high temperature (>−10°C), it is still difficult to increase the toughness of the blends at lower temperatures [Figure 5(b)]. Furthermore, for the purpose of comparison, the curves of R/C/0.05G blends with high IPC content (20∼40 wt %) are also given in Figure 5(c,d). Very interestingly, besides the decrease of B–D transition temperature and the acceleration of the transition process, a good low-temperature impact toughness is obtained when the content of IPC exceeds 20 wt %. The above results indicate that the synergistic toughening of IPC and WBG at low temperature is efficient if enough amounts of IPC and WBG (20 wt % for IPC and 0.1 wt % for WBG) are added into PPR matrix.

The stress–strain curves of PPR/IPC/WBG blends are shown in Figure 6 and the related mechanical parameters are listed in Table II. Obviously, although there is a slight decrease in the Young's modulus and yield strength after adding IPC and WBG, the elongation at break shows a great improvement. Most importantly, compared with PP toughened with traditional elastomers, such as EPDM, POE etc.,[26,27] where the enhancement of toughness is always companied with a great deterioration of strength, the significantly improved impact toughness of PPR/IPC/WBG blends with little loss of strength and stiffness is very important from the viewpoint of industrial application.

Polycrystalline Composition and Phase Morphology of PPR/IPC/WBG Blends as a Function of IPC Content and WBG Content

The effects of IPC content and WBG content on the relative amount of β-form crystals in PPR/IPC/WBG blends were

Table I. Values of K_β and X_c Obtained by WAXD Measurements for the Samples

Samples	K_β (%)	X_c (%)
R	0	43
R/10C	0	44
R/0.05G	34	45
R/10C/0.05G	72	48

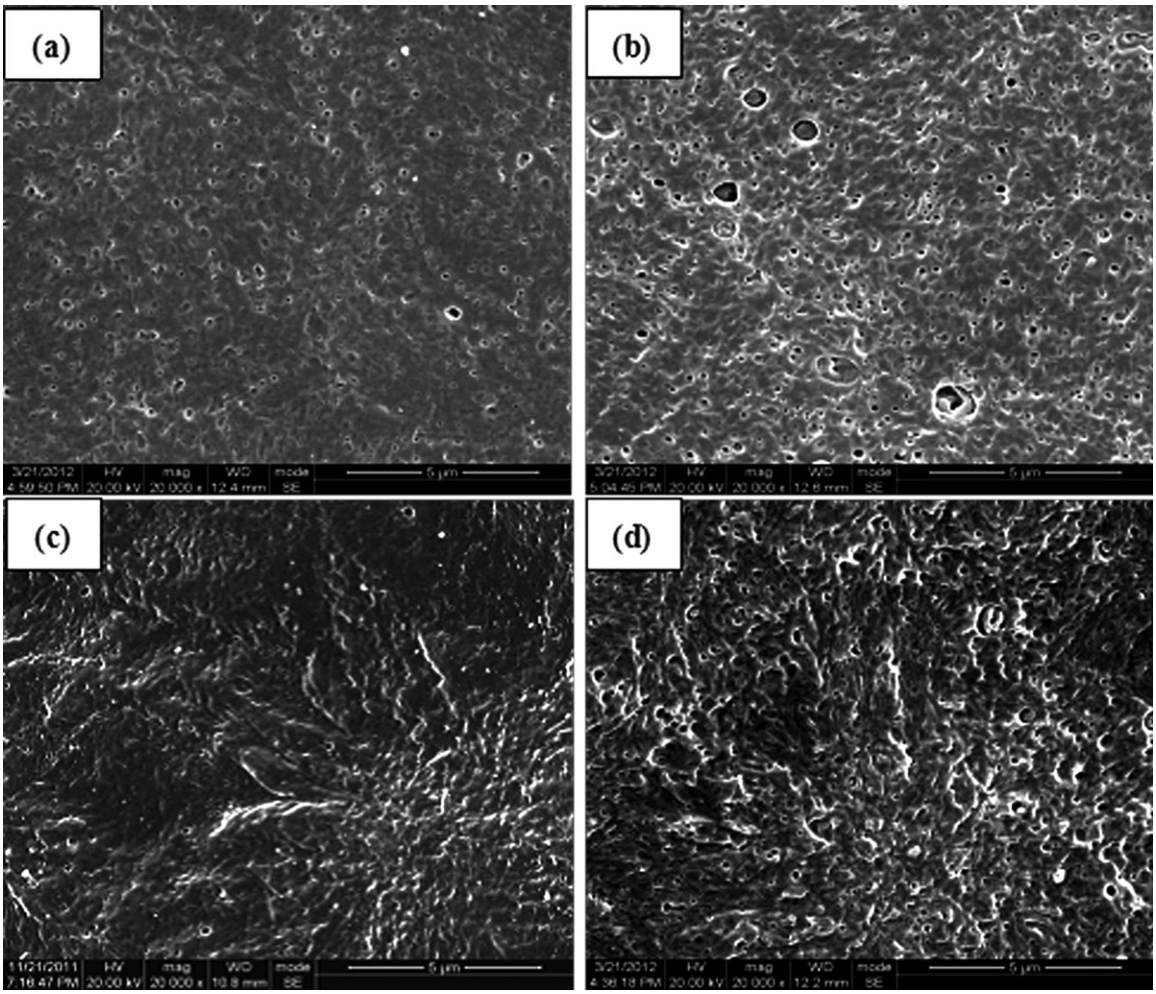

Figure 4. SEM micrographs of the samples: (a) PPR, (b) PPR/10IPC, (c) PPR/0.05WBG, and (d) PPR/10IPC/0.05WBG.

investigated by WAXD. The WAXD spectra of the blends are shown in Figure 7, and the values of K_β and X_c are summarized in Table III. It is interesting to find that the presence of 10 wt % IPC in β-nucleated PPR gives rise to an evident increase in the content of β-form crystals, but further increasing the content of IPC doesn't induce the further enhancement in the relative amount of β-form crystals, suggesting that there is a saturation content of IPC for the improvement of β-crystallization capability of PPR with WBG. For R/10C blend nucleated with different WBG contents, it is found that there exists a critical nucleation concentration (0.05∼0.1 wt %). The value of K_β decreases slightly with increasing WBG content from 0.1 to 0.2 wt %. Similar phenomenon has been reported in the literature and it is ascribed to the difference in solubility and nucleating duality of β-NA.36 At high concentration (e.g., $>$ 0.1 wt %), the agglomeration of β-NA and the decrease of β-nucleating ability would lead to the loss of β-nucleating efficiency. In addition, there is no obvious difference in the values of X_c for all the blends with different contents of IPC and WBG.

Figure 8 shows the microstructures of PPR/IPC and PPR/IPC/0.05WBG blends with different IPC contents. As expected, both the number and the size of rubbery EPR phase increase apparently with increasing IPC content [Figure 8(a,b)]. More interestingly, it is clearly observed that the phase morphology of PPR/IPC/0.05WBG blends is distinctly different from that of PPR/IPC blends. As shown in Figure 8(b,d), the EPR rubbery phase becomes smaller and more uniform with the addition of 0.05 wt % WBG into PPR/40IPC blend because of the suppressing effect of β-NA nucleated matrix crystallization on the phase separation as mentioned earlier, which is favorable to the toughening because the matrix ligament thickness is expected to decrease in this case.[37] On the other hand, much more granules are formed in the β-nucleated PPR/40IPC blend as compared with PPR/40IPC blend. In a previous work,[38] we have demonstrated that this phenomenon is closely related to the largely enhanced crystallization of IPC in the presence of β-NA and the formation of such PE-rich granules is indicative of strong interaction between the EPR dispersed phase and the PP matrix. Obviously, the addition of WBG in the blends can not only control the crystalline structure but also tailor the phase structure effectively. Similar results have been reported in Bai's work.[31]

Synergistic Toughening Mechanism

As discussed above, the greatly improved impact toughness in the blends of PPR/IPC/0.05 WBG is mainly attributed to the

Applied Polymer SCIENCE

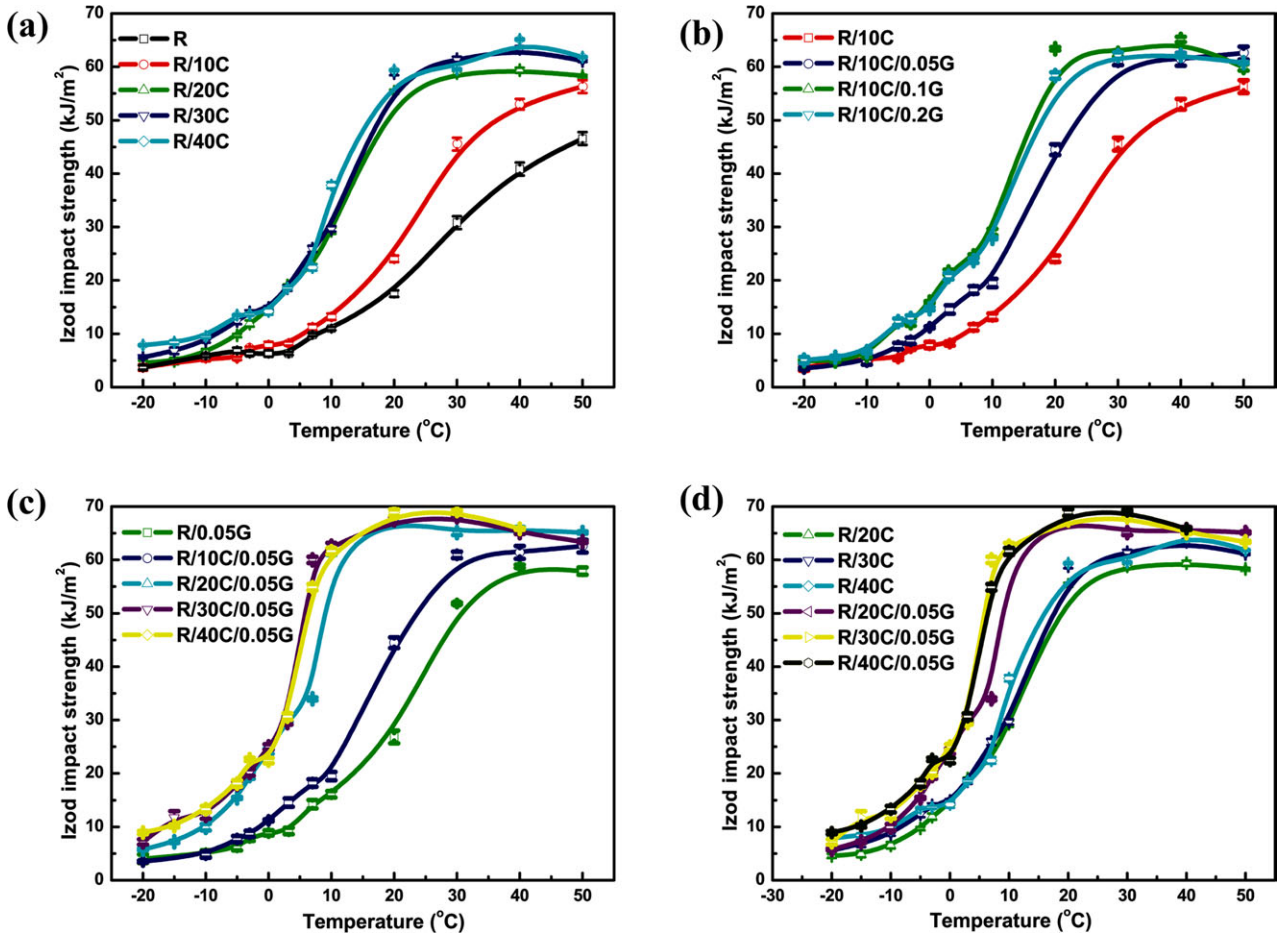

Figure 5. Brittle–ductile transition curves of the samples: (a) PPR/IPC blends with different IPC contents, (b) PPR/10IPC/WBG blends with different WBG contents, (c) PPR/IPC/0.05WBG blends with different IPC contents, and (d) PPR/IPC blends with and without WBG. [Color figure can be viewed in the online issue, which is available at wileyonlinelibrary.com.]

combined effect of polycrystalline composition and multiphase morphology. Shearing yielding of matrix is the main energy dissipation mechanism for elastomer toughened polymer blends.[39] The easier the shearing yielding, the better is the impact toughness. Compared with α-form crystals with cross-hatched structure, the WBG induced β-form crystals with loose structure allow the shear yielding of PPR matrix becoming more easily even at relative low temperature. On the other hand, the

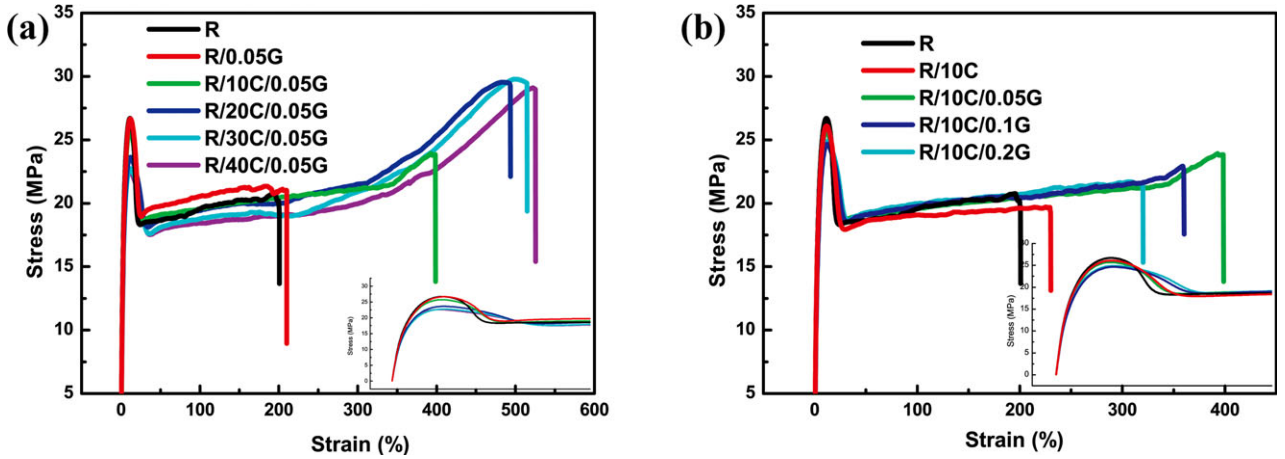

Figure 6. Stress–strain curves of (a) PPR/IPC/WBG blends with different IPC contents and (b) those with different WBG contents. [Color figure can be viewed in the online issue, which is available at wileyonlinelibrary.com.]

Table II. Values of Yield Strength, Young's Modulus, and Elongation at Break for the Samples

Samples	Yield strength (MPa)	Young's modulus (MPa)	Elongation (%)
R	26.7 ± 0.3	872 ± 19	200 ± 2
R/10C	26.1 ± 0.3	863 ± 40	230 ± 47
R/0.05G	26.7 ± 0.3	854 ± 13	210 ± 25
R/10C/0.05G	25.7 ± 0.2	861 ± 20	398 ± 50
R/10C/0.1G	24.6 ± 0.4	795 ± 2	360 ± 23
R/10C/0.2G	24.9 ± 0.2	821 ± 3	320 ± 23
R/20C/0.05G	23.6 ± 0.2	804 ± 8	493 ± 19
R/30C/0.05G	22.7 ± 0.2	786 ± 13	515 ± 25
R/40C/0.05G	22.6 ± 0.1	821 ± 8	525 ± 5

presence of IPC in the blends not only promotes the formation of β-form crystals but also acts as an elastomer to toughen PPR. In addition, the largely improved multiphase structure induced by adding β-NA also contributes to the enhancement in the toughness. By this way, WBG and IPC show a synergistic toughening effect on PPR.

It has been long known that the fracture toughness is the substantial response of molecular mobility. To gain a deeper understanding on the toughening mechanism, the molecular mobility of the blends was also investigated using DMA. Figures 9 and 10 show the curves of the mechanical loss factor as a function of temperature. All the curves exhibit three different damping peaks: the peak around −45°C is associated with the glass transition of the rubbery EPR phase; the other two peaks at around 10 and 70°C are related to the β-relaxation of basal PP phase (i.e., glass transition of unconstrained amorphous chains) and α-relaxation of basal PP phase (i.e., glass transition of rigid amorphous chains), respectively.[40,41] Clearly, no obvious changes in the intensity of EPR-relaxation can be observed with the addition of WBG into PPR/10IPC, suggesting that the presence of β-NA dose not influence the molecular mobility of EPR

Table III. Values of K_β and X_c Obtained by WAXD for the Samples

Samples	K_β (%)	X_c (%)
R/10C/0.05G	72	48
R/20C/0.05G	66	47
R/30C/0.05G	66	46
R/40C/0.05G	65	48
R/10C/0.1G	73	47
R/10C/0.2G	59	50

phase [Figures 9 and 10(a)]. However, the intensity of β-relaxation increases apparently after adding small amounts of β-NA [Figure 10(a)], indicating that the mobility of amorphous chains in β-form crystals is higher than that in α-form crystals. This is critical in improving the matrix toughness of β-nucleated blends. From Figure 10(b), one can see that the intensity of EPR-relaxation enhances with increasing IPC content form 10–30 wt %. This can be explained by the increased EPR phase content. The concentration of ethylene component in IPC (13.5 wt %) is much higher than that in PPR (3.8 wt %). Above all, from the viewpoint of molecular mobility, the addition of IPC and WBG in PPR can promote the relaxation of dispersed rubbery EPR phase and β-relaxation of matrix simultaneously and finally results in the significant enhancement in impact toughness.

CONCLUSIONS

The addition of IPC and β-NA simultaneously can greatly improve the impact toughness of PPR, evidenced by the shift of B–D transition towards lower temperatures and the accelerated transition. The reason for these changes can be explained from three aspects. First, the significantly increased relative amount of β-form PPR with the addition of β-NA and IPC will decrease the yield stress of PPR matrix. In addition, as the IPC content increases, the content and the relaxation intensity of EPR phase increase, thus more stress concentration center and energy

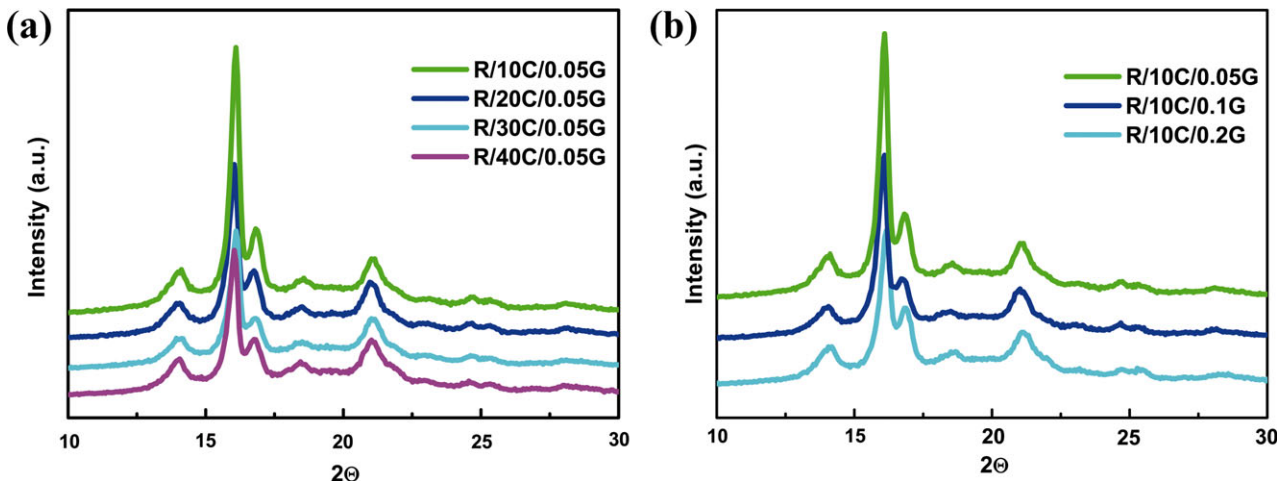

Figure 7. WAXD spectra of (a) PPR/IPC/WBG blends with different IPC contents and (b) those with different WBG contents. [Color figure can be viewed in the online issue, which is available at wileyonlinelibrary.com.]

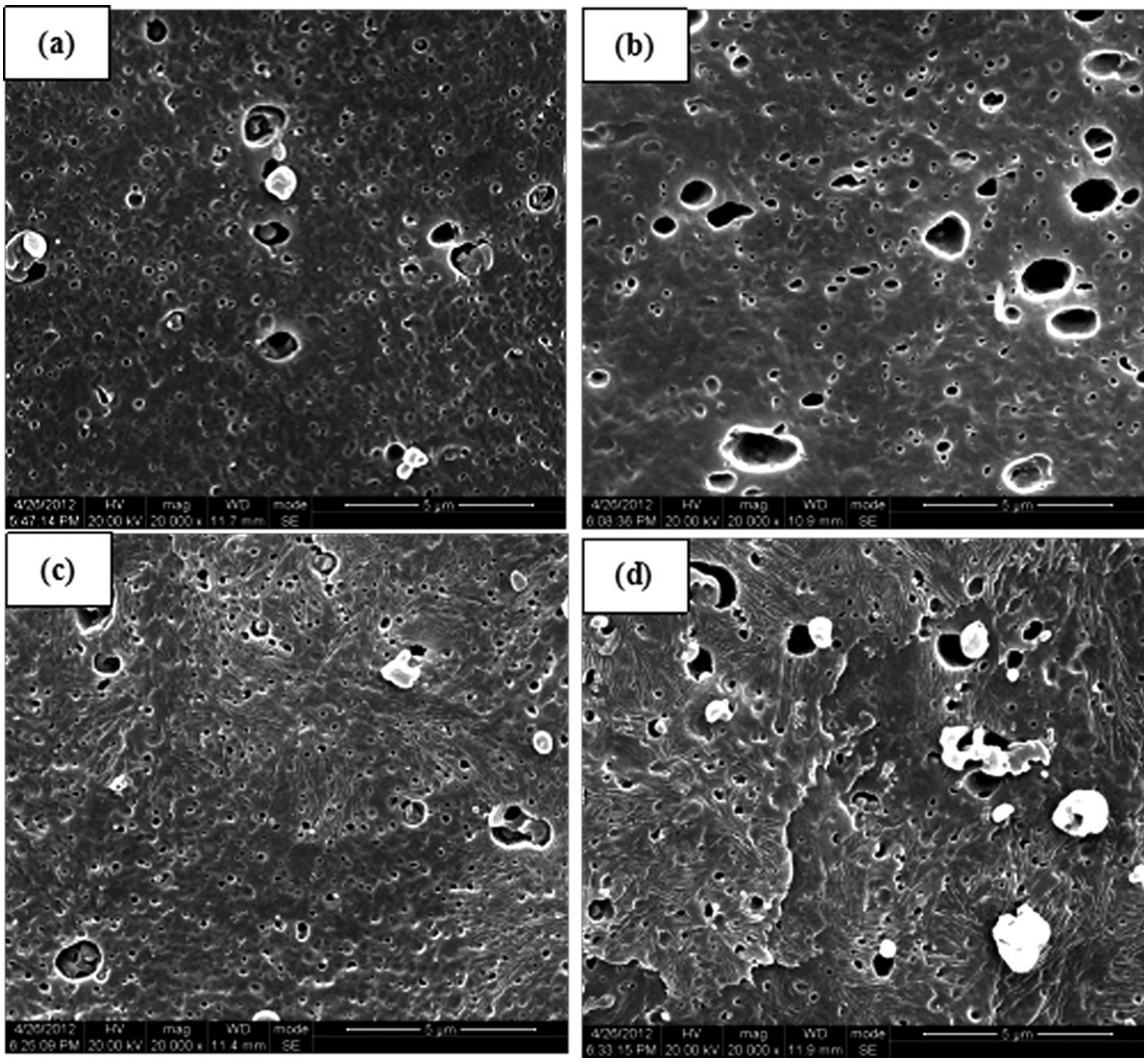

Figure 8. SEM micrographs of the samples: (a) PPR/20IPC, (b) PPR/40IPC, (c) PPR/20IPC/0.05WBG, and (d) PPR/40IPC/0.05WBG.

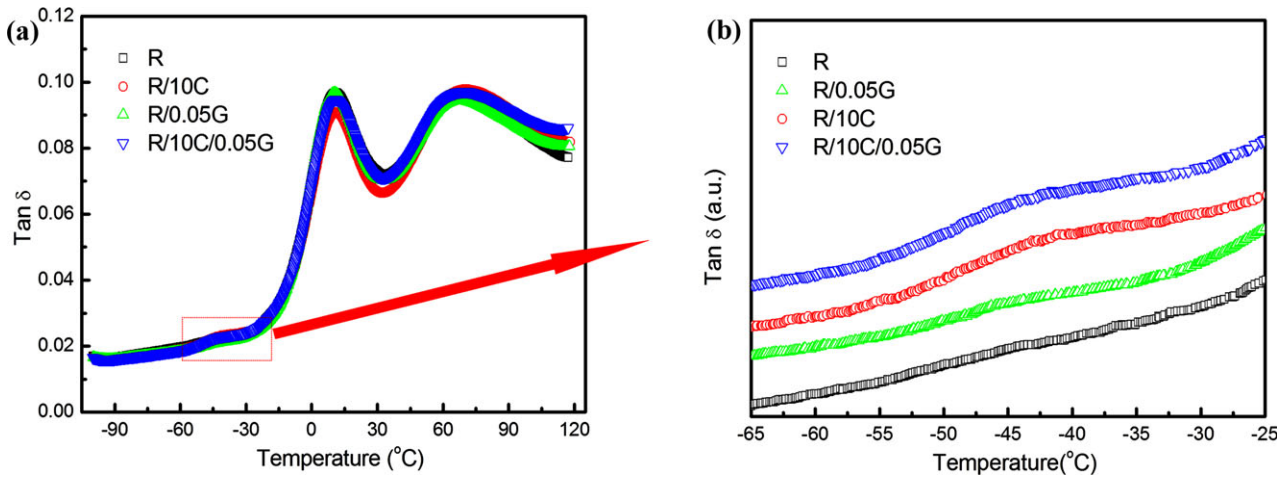

Figure 9. Comparison of mechanical loss factor of PPR, PPR/10IPC, PPR/0.05WBG, and PPR/10IPC/0.05WBG. [Color figure can be viewed in the online issue, which is available at wileyonlinelibrary.com.]

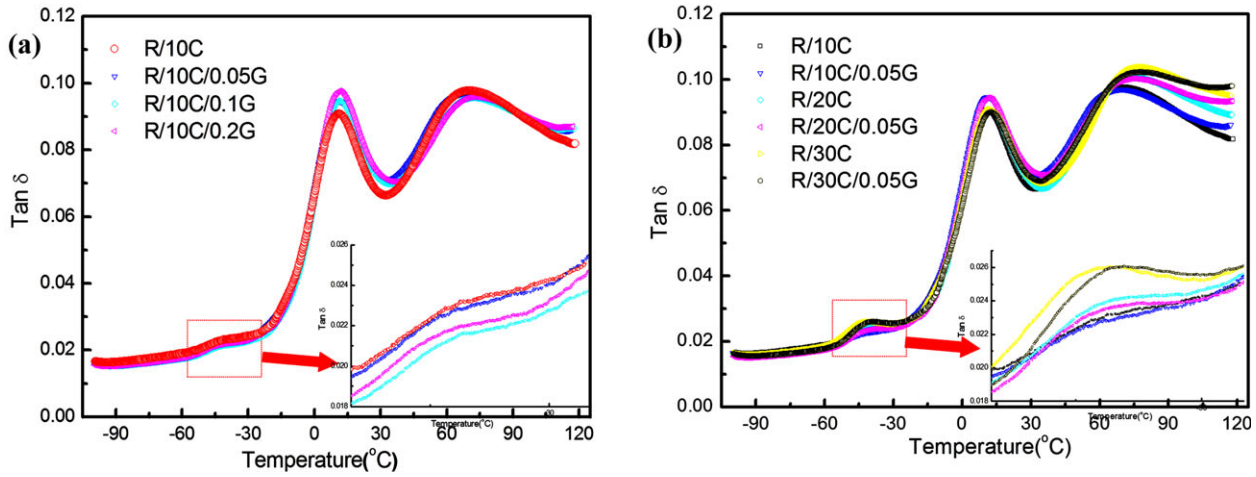

Figure 10. Comparison of mechanical loss factor of (a) PPR/IPC/WBG blends with different IPC contents and (b) those with different WBG contents. [Color figure can be viewed in the online issue, which is available at wileyonlinelibrary.com.]

dissipation are available. Finally, the improved dispersion of rubbery phase in PPR/IPC blends by adding WBG will decrease the ligament thickness and then promote the shear yielding of the matrix. In summary, there is a synergistic effect of IPC and β-NA on the improvement in the toughness of PPR.

ACKNOWLEDGMENTS

This work was supported by the Special Funds for Major State Basic Research Projects of China (2011CB606006), and National Natural Science Foundation of China (51121001, 50903048).

REFERENCES

1. McNally, T.; McShane, P.; Nally, G.; Murphy, W.; Cook, M.; Miller, A. *Polymer* **2002**, *43*, 3785.
2. Silvestre, C.; Cimmino, S.; Triolo, R. *J. Polym. Sci. Part B: Polym. Phys.* **2003**, *41*, 493.
3. Luo, F.; Wang, K.; Wang, J. W.; Deng, H.; Zhang, Q.; Chen, F.; Fu, Q.; Na, B. *Polym. Int.* **2011**, *60*, 1705.
4. Luo, F.; Wang, J. W.; Bai, H. W.; Wang, K.; Deng, H.; Zhang, Q.; Chen, F.; Fu, Q.; Na, B. *Mater. Sci. Eng. A* **2011**, *528*, 7052.
5. Wang, R. H.; Qu, Y. Q. *Techno.-Econ.* **2007**, *23*, 39.
6. Satapathy, B. K.; Das, A.; Patnailk, A. *J. Mater. Sci.* **2011**, *46*, 1963.
7. Fu, Z.; Dai, W. L.; Yu, H. M.; Zou, X. X.; Chen, B. Q. *J. Mater. Sci.* **2011**, *46*, 1272.
8. Brostow, W.; Datashvili, T.; Geodakyan, J.; Lou, J. *J. Mater. Sci.* **2011**, *46*, 2445.
9. Xie, X. L.; Li, R. K. Y.; Tjong, S. C.; Mai, Y. W. *Polym. Compos.* **2002**, *23*, 319.
10. Malkapuram, R.; Kumar, V.; Negi, Y. S. *J. Reinf. Plast. Comp.* **2009**, *28*, 1169.
11. Jiang, W.; Yu, D.; An, L.; Jiang, B. *J. Polym. Sci. Part B: Polym. Phys.* **2004**, *42*, 1433.
12. Li, J.; Zhang, X.; Qu, C.; Zhang, Q.; Du, R. N.; Fu, Q. *J. Appl. Polym. Sci.* **2007**, *105*, 2252.
13. Stehling, F. C.; Huff, T.; Speed, C. S.; Wissler, G. *J. Appl. Polym. Sci.* **1981**, *26*, 2693.
14. Paul, S.; Kale, D. D. *J. Appl. Polym. Sci.* **2000**, *76*, 1480.
15. Tam, W. Y.; Cheung, T.; Li, R. K. Y. *Polym. Test.* **1996**, *15*, 363.
16. Shangguan, Y. Y.; Song, Y. H.; Peng, M.; Li, B. P.; Zheng, Q. *Eur. Polym. J.* **2005**, *41*, 1766.
17. Luo, F.; Xu, C. L.; Wang, K.; Deng, H.; Chen, F.; Fu, Q. *Polymer* **2012**, *53*, 1783.
18. Zheng, Q.; Shangguan, Y. Y.; Yan, S. K.; Song, Y. H.; Peng, M.; Zhang, Q. B. *Polymer* **2005**, *46*, 3136.
19. Huo, H.; Jiang, S. C.; An, L. J. *Macromolecules* **2004**, *37*, 2478.
20. Rajkiran, R.; Tiwari, D. R.; Paul. *Polymer* **2012**, *53*, 823.
21. Yi, Q. F.; Wen, X. J.; Dong, J. Y.; Han, C. C. *Polymer* **2008**, *49*, 5053.
22. Luo, F.; Geng, C. Z.; Wang, K.; Deng, H.; Chen, F.; Fu, Q.; Na, B. *Macromolecules* **2009**, *42*, 9325.
23. Varga, J. *J. Macro. Sci. Part B* **2002**, *41*, 1121.
24. Varga, J. *J. Therm. Anal.* **1989**, *35*, 1891.
25. Christelle, G. *Adv. Polym. Sci.* **2005**, *188*, 43.
26. D'Aniello, C.; Guadagno, L.; Gorrasi, G.; Vittoria, V. *Polymer* **2000**, *41*, 2515.
27. Min, S. S.; Lee, S. S.; Jho, J. Y. *Polym. Test.* **2001**, *20*, 855.
28. Pang, Y. Y.; Dong, X.; Liu, K. P.; Han, C. C.; Chen, E. Q.; Wang, D. J. *Polymer* **2008**, *49*, 4259.
29. Vader, W. A.; Mulder, J. J.; Oderkerk, J.; Gaymans, R. J. *Polymer* **1998**, *39*, 6781.
30. Bai, H. W.; Wang, Y.; Song, B.; Li, Y. L.; Liu, L. *J. Polym. Sci. Part B: Polym. Phys.* **2008**, *46*, 577.
31. Bai, H. W.; Wang, Y.; Song, B.; Han, L. *J. Appl. Polym. Sci.* **2008**, *108*, 3270.

32. Bai, H. W.; Wang, Y.; Song, B.; Huang, T.; Han, L. *J. Polym. Sci. Part B: Polym. Phys.* **2009**, *47*, 46.

33. Grein, C.; Gahleitner, M. *Express Polym. Lett.* **2008**, *2*, 392.

34. Luo, F.; Zhu, Y. L.; Wang, K.; Deng, H.; Chen, F.; Zhang, Q.; Fu, Q. *Polymer* **2012**, *53*, 4861.

35. Turner-Jones, A.; Aizlewood, J.; Beckett, D. *Macromol. Chem. Phys.* **1964**, *75*, 134.

36. Luo, F.; Wang, K.; Ning, N. Y.; Geng C. Z.; Deng, H.; Chen, F.; Fu, Q.; Qian, Y. Y.; Zheng, D. *Polym. Adv. Technol.* **2011**, *22*, 2044.

37. Yang, J. H.; Zhang, Y.; Zhang, Y. X. *Polymer* **2003**, *44*, 5047.

38. Zhang, C.; Shangguan, Y.; Chen, R.; Wu, Y.; Chen, F.; Zheng, Q. *Polymer* **2002**, *51*, 4969.

39. Estevez, R.; Tijssens, M. G. A.; Van der Giessen, E. *J. Mech. Phys. Solids* **2000**, *48*, 2585.

40. Karger-Kocsis, J. *Polym. Eng. Sci.* **1987**, *27*, 254.

41. Jafari, S. H.; Gupta, A. K. *J. Appl. Polym. Sci.* **2000**, *78*, 962.